International Journal of Advance Scientific Research
(ISSN – 2750-1396)
VOLUME 03 ISSUE 04 Pages: 78-82
SJIF IMPACT FACTOR (2021: 5.478) (2022: 5.636) (2023: 6.741)
OCLC – 1368736135
ISSN-2750-1396


ISSN 2750-1396
SJIF 2023-6.741
INTERNATIONAL JOURNAL OF ADVANCE SCIENTIFIC RESEARCH
IJASR
VOLUME 03
2023

Journal Website: http://sciencebring.com/index.php/ijasr

Research Article

MATHEMATICAL MODEL OF TWO-WAVE OPTOELECTRONIC DEVICE FOR REMOTE MONITORING OF EXPLOSIVE HYDROCARBONS CONCENTRATION

Submission Date: April 19, 2023, **Accepted Date:** April 24, 2023,
Published Date: April 29, 2023
Crossref doi: https://doi.org/10.37547/ijasr-03-04-11

U.M. Mirzaeva
Fergana State University, Fergana, Uzbekistan

X.T. Yoldashev
Fergana Polytechnic Institute, Fergana, Uzbekistan

ABSTRACT

The demand for hydrocarbons in industrial production enterprises and people's daily life is increasing day by day. In the same way, the oil refining and gas industries are developing very rapidly in all developed countries of the world. But today, small-scale, high-sensitivity, high-selectivity, and high-speed remote monitoring of explosive concentrations of hydrocarbons in the atmosphere are being developed.

KEYWORDS

Mathematical model, high-selectivity, high-speed remote monitoring, comparator device, explosive concentrations.

INTRODUCTION

The lack of gas analysers causes several problems. Accumulation of explosive concentrations of hydrocarbons in the air often endangers human life and also leads to man-made losses [1-4]. Therefore, today it is of great importance to create and research small-sized, high-sensitivity, high-selectivity, and high-speed gas analysers that automatically monitor explosive concentrations of hydrocarbons in the atmosphere.

The block diagram of the two-wave optoelectronic device for remote monitoring of the explosive concentration of hydrocarbons is shown in Fig. 1. Here: BG - control generator, T - trigger; CHB - frequency divider; EM – exponential modulator; EQ – emitter-return converter; IK - pulse amplifier; ND1 – base light diode; ND2 - measuring light diode; L is the distance to the control object; DK1 and DK2 - first and second differentiating devices; NO - object of control; FP - photoreceiver; KSHK - low-noise amplifier; TKK - comparator device; XS – counter; DSH - decoder; IN – indicator [5-6].

Time diagrams representing the principle of operation of the two-wave optoelectronic device for remote monitoring of the potentially explosive concentration of hydrocarbons are presented in Figures 1 and 2.

THE MAIN PART

The optoelectronic device works as follows: the control generator BG produces right-angled pulses with a frequency sequence of 2000.0 Hz (Fig. 2.a). The resulting pulses affect the input of the trigger T. At its output, rectangular pulses with a frequency of 1000.0 Gs are generated (Fig. 2, b, v), and they affect the input of the frequency divider CHB, and its output has a frequency of 10 Gs. mipulses are formed (Fig. 2, g). Right-angle pulses are fed from the output of the frequency divider to the first input of the exponential modulator, and right-angle pulses from the trigger output to the second input. As a result, discrete pulses are generated at the output of the exponential modulator, the amplitude of which decreases exponentially with time. These pulses are amplified by the emitter-return EQ and fed to the input of the base light diode ND1. Discrete exponential pulses with inverse phase are fed from the trigger output to the input of the pulse amplifier IK. Its output is amplified in amplitude and fed to the input of the measuring light diode ND2, which is divided into discrete exponential pulses. The resulting measurement and reference light fluxes are directed to the control object NO - located at a distance L, and the light fluxes returned from the control object are received by the photoreceptor FP (Fig. 1, d).

The light currents falling on the surface of the photoreceptor are determined as follows.

$$\varPhi_{\lambda 1}=\gamma_{\lambda 1} I_{0\lambda 1}\frac{S_{\varPhi\Pi}}{L^2}e^{-k_1N_1} \qquad (1)$$

$$\varPhi_{\lambda 2}=\gamma_{\lambda 2} I_{0\lambda 2}\frac{S_{\varPhi\Pi}}{L^2}e^{-k_2N_1}e^{-k_3N_2} \qquad (2)$$

where: and - return coefficients of the control object corresponding to the measurement and reference wavelengths; and - light intensity corresponding to the measurement and reference light fluxes returned from the control object; - the surface of the photoreceptor entrance slot; L is the distance to the control object; - the total concentration of gaseous substances collected in the control facility; - explosive concentration of hydrocarbons.

It should be mentioned that the intensity of the initial base beam changes exponentially with time, i.e.

$$\Phi_{\lambda 2} = \gamma_{\lambda 2} I_{0\lambda 2} \frac{S_{\Phi\Pi}}{L^2} e^{-k_2 N_1} e^{-k_3 N_2} \qquad (3)$$

Where: A is the amplitude of the initial base beam current; - time; - the time constant of the exponential pulse.

That's why the base beam falling on the photoreceptor is shown below

$$\Phi_{\lambda 1} = A\gamma_{\lambda 1} I_{0\lambda 1} \frac{S_{\Phi\Pi}}{L^2} e^{-k_1 N_1} e^{-\frac{t}{\tau}} \qquad (4)$$

At the equalization time of the measuring and reference beam currents, i.e. = , we have the following

$$A\gamma_{\lambda 1} \frac{S_{\Phi\Pi}}{L^2} e^{-k_1 N_1} e^{-\frac{t_{CP}}{\tau}} = \gamma_{\lambda 2} I_{0\lambda 2} \frac{S_{\Phi\Pi}}{L^2} e^{-k_2 N_1} e^{-k_3 N_2} \qquad (3)$$

here: t_{CP} - $\Phi_{\lambda 1}$ va $\Phi_{\lambda 2}$ equalized time of light fluxes.

If the wavelengths of the reference and measuring light currents are chosen close to each other, then the reflection and scattering coefficients corresponding to the reference and measuring wavelengths will be equal, i.e.

$$\gamma_{\lambda 1} = \gamma_{\lambda 2},\ k_1 = k_2 .$$

Therefore, if the initial values of the measurement and reference beam currents are equal, we have.

$$e^{-\frac{t_{CP}}{\tau}} = e^{-k_3 N_2} \qquad (4)$$

from this

$$N_2 = \frac{1}{k_2 \tau} t_{CP} \qquad (5)$$

As can be seen from the last equation, the time of measurement of the explosive concentration of hydrocarbons and the equalization of the base beam currents

t_{CP} because it is proportional to $\frac{1}{k_2 \tau}$ magnitude is a constant constant number.

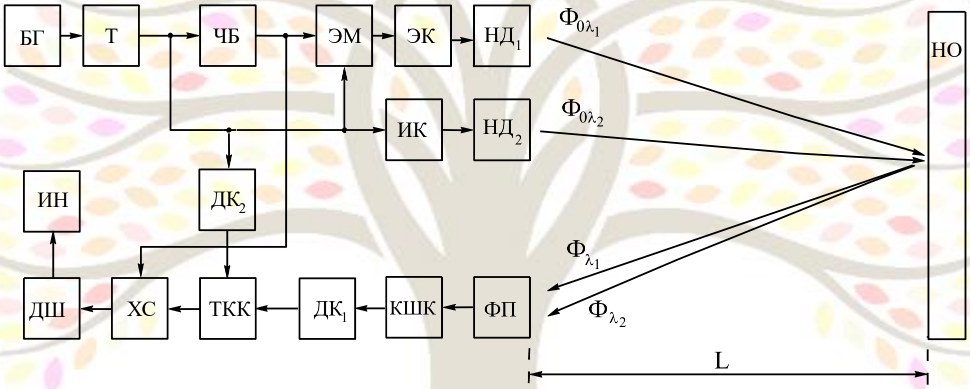

Fig. 1. Block diagram of the optoelectronic device for remote monitoring of the explosive concentration of hydrocarbons

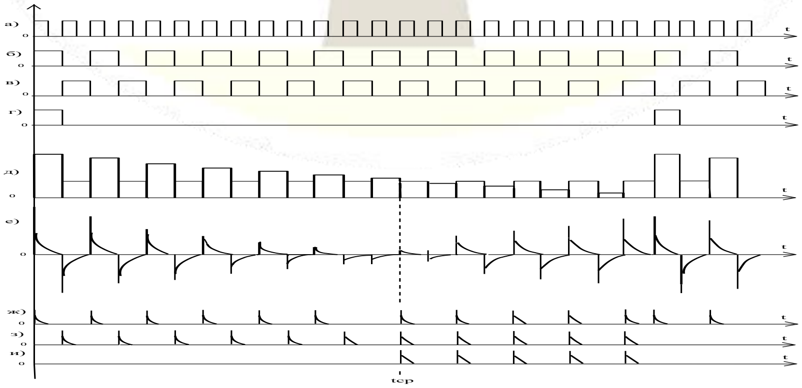

Fig. 2. Timing diagram representing the principle of operation of the optoelectronic device that remotely monitors the explosive concentration of hydrocarbons.

To implement the processes described above, the photoelectric signal at the output of the photoreceptor is amplified using a low-noise amplifier, differentiated in the first differentiating device (Fig. 2, e, j) and then fed to the first input of the comparator device. And the second input of the comparison gate TQQ received differentiated pulses in the second differentiating device (Fig. 2,z). As a result, a series of pulses proportional to the explosive concentration of hydrocarbons is formed at the output of the comparator (Fig. 2,i). These pulses are counted in the counter XS and displayed on the indicator using appropriate decoders. Thus, depending on the indicators, the explosive concentration of hydrocarbons is determined.

REFERENCES

1. Juraboyev, N. I., & Yuldashev, K. T. (2022). Analysis of energy saving techniques of home appliances. American Journal of Applied Science and Technology, 2(05), 61-66.
2. Tojimatov, S. S., & Yuldashev, K. T. (2022). Designing of the automated control system of liquid level in the tank sizes specified. International Journal of Advance Scientific Research, 2(05), 51-58.
3. Khamdamov, D. H., & Yuldashev, K. T. (2022). Using modern automation in the greenhouse. International Journal of Advance Scientific Research, 2(05), 28-37.
4. Abdumalikova, Z. I. (2021). Metrological provision in the production and its branches. Asian Journal of Multidimensional Research, 10(10), 1492-1496.
5. Abdumalikova, Z. I. (2021). Manifestation of Sources of Uncertainty in Measurements. Central Asian Journal of Theoretical and Applied Science, 2(12), 301-305.
6. Madmarova, U. A., & Abdumalikova, Z. I. (2022). The design of printed board drawings. American Journal of Applied Science and Technology, 2(07), 15-22.